

Development of the Q=10 Scenario for ITER on ASDEX Upgrade (AUG)

J. Schweinzer 1), M. Beurskens 1), L. Frassinetti 2), E. Joffrin 3), V. Bobkov 1), R. Dux 1), R. Fischer 1), C. Fuchs 1), A. Kallenbach 1), C. Hopf 1), P.T. Lang 1), A. Mlynek 1), T. Pütterich 1), F. Ryter 1), J. Stober 1), G. Tardini 1), E. Wolfrum 1), H. Zohm 1) the EUROfusion MST1 Team *) and the ASDEX Upgrade Team

1) Max Planck Institute for Plasma Physics, 85748 Garching, Germany

2) KTH, Division of Fusion Plasma Physics, SE-10044 Stockholm, Sweden

3) CEA, Centre de Cadarache, 13108 Saint Paul-lez-Durance, France

*) See <http://www.euro-fusionscipub.org/mst1>.

E-mail contact of main author: josef.schweinzer@ipp.mpg.de

Abstract. The development of the baseline H-mode scenario foreseen for ITER on the ASDEX Upgrade tokamak, i.e. discharges at $q_{95}=3$, relatively low $\beta_N \sim 1.8$, high normalized density $n/n_{GW} \sim 0.85$ and high triangularity $\delta=0.4$, focused on the integration of elements foreseen for ITER and available on ASDEX Upgrade, such as ELM mitigation techniques and impurity seeding in combination with a metallic wall. Values for density and energy confinement simultaneously came close to the requirements of the ITER baseline scenario as long as β_N stayed above 2. At lower heating power and thus lower β_N normalized energy confinement $H_{98y2} \sim 0.85$ is obtained. It has been found that stationary discharges are not easily achieved under these conditions due to the low natural ELM frequency occurring at the low q_{95} / high δ operational point. Up until now the ELM parameters were uncontrollable with the tools developed in other scenarios. Therefore studies on an alternative operational point at higher β_N and q_{95} have been conducted. In order to prepare for the ITER first non-activation operational phase, Helium operation has been investigated as well.

1. Introduction

In ITER, H-mode operation at 15MA and $q_{95}=3$ is planned to achieve 500MW fusion power at Q=10 in deuterium-tritium mixtures. This so-called ITER baseline (BL) scenario is

characterized by normalized parameters for plasma density $f_{\text{GW}}=n/n_{\text{GW}}=0.85$, energy confinement $H_{98y2}\sim 1$ and beta $\beta_N\sim 1.8$ [1]. Based on results from tokamaks with a carbon wall, a high triangularity shape ($\delta=\delta_{\text{average}}\sim 0.4$) has been identified to be best suited in ITER to combine high density operation using continuous deuterium gas puffing with good H-mode confinement [2 and references therein]. In recent years experimental demonstration of the ITER BL scenario has been studied on devices like Alcator C-Mod, DIII-D and JET [3, 4, 5, 6]. These experiments were conducted with three different types of plasma facing material, molybdenum, carbon and beryllium plus tungsten, but no case with full tungsten walls. So the ASDEX Upgrade (AUG) experiments presented in this paper provide a complementary set of data in this respect and were conducted with the aim of matching plasma shape and parameters like H_{98y2} , β_N and f_{GW} as closely as possible to those of ITER.

The all-tungsten wall of AUG requires central wave-heating (ECRH or ICRF) to avoid core tungsten impurity accumulation. This boundary condition of needing RF power centrally deposited in the plasma, limits the possible values for plasma current I_p and magnetic field B_t to a few practical combinations of I_p / B_t . In particular, two routes [7] have been explored for $q_{95}=3$ plasmas on AUG: (i) operation at 1.1MA/1.8T using ECRH at 140GHz in X3 mode and (ii) 1.2MA/2T using ICRH at 30MHz from two antennas with boron-coated protection limiter tiles.

This paper will discuss the present status of ITER BL demonstration plasmas on AUG based on experiments carried out between 2012 and 2014 and will describe attempts to mitigate ELMs in this scenario as well as propose a slight shift of the scenario's operational point towards a potential 'less difficult corner' at 20% lower I_p (higher q_{95}).

2. Behaviour of $q_{95}=3$ ITER BL discharges on AUG

A typical example for the demonstration of the ITER BL scenario at 1.2MA / 2T can be seen in fig. 1. Such discharges are typically ramped up to 1MA in a low- δ shape, followed by a combined slow ramp of I_p and δ until the flattop is reached and sustained for 2 to 3 seconds. The discharges are dominantly fuelled by gas valves in the divertor. The feed-forward gas fuelling rate is slowly raised up to a flattop value of typically $\sim 2.5 \cdot 10^{22}$ atoms/s. Such a puff rate corresponds to a divertor neutral pressure of about 1.7Pa. In several discharges stationary behaviour is obtained in the flattop and parameters H_{98y2} and f_{GW} simultaneously come close to the target values of 1 and 0.85, respectively [7, 8]. Although the amount of applied heating power in the standard heating recipe for such discharges is already at the lower end for AUG,

β_N typically stays at values 20% above the ITER target of 1.8. Thus, in ITER BL plasma on AUG normally too much additional heating power is applied, which is on the other hand helpful for an effective impurity flushing by ELMs because f_{ELM} stays sufficiently high.

During the ramp-up of I_p and δ , the ELM signature of such ITER BL discharges changes. While in the early phase (low δ , $q_{95} \sim 3.5$) the ELM frequency f_{ELM} is high at 100Hz, and the energy loss per ELM ΔW_{ELM} at 20-40 kJ is low, the situation reverses once both parameters δ and q_{95} approach their flattop values of 0.36 and 3 respectively. In the fully shaped flattop low ELM-frequencies of 10 - 25 Hz are typical as well as large energy losses ΔW_{ELM} values of 40 – 120 kJ, which means 5% – 15% losses of stored energy per ELM event which are intolerable in view of ITER [9].

The operational window for the ITER BL scenario on AUG where a stationary behaviour is possible and W accumulation can be avoided is set by the following (inter-linked) parameters:

- Closeness to the last boronization / quality of wall conditioning [10];
- Deuterium gas puff level;
- Heating power in total and in particular the amount centrally deposited;

The D gas puff level and the heating power are important parameters to keep the ELM frequency f_{ELM} sufficiently high to allow an effective flushing of impurities necessary to avoid W accumulation. With well conditioned walls, i.e. a few days after a boronization, the gas puff level could be reduced to $1.5 \cdot 10^{22} \text{ s}^{-1}$ being then close to the onset of W accumulation. Many stationary discharges were conducted with a safety margin in order to prevent W accumulation at D puff levels between $2 \cdot 10^{22} \text{ s}^{-1}$ and $3 \cdot 10^{22} \text{ s}^{-1}$. Only in such phases with well conditioned walls could ITER BL ($I_p = 1.1$ or 1.2 MA) discharges with $P_{\text{NBI}} < 5\text{MW}$ be sustained, or the central RF heating could be reduced to low values of less than 1MW. At a heating power just slightly above the H-mode power threshold, W accumulation and a subsequent radiative collapse becomes likely even with well conditioned walls.

For ITER BL attempts where the beneficial effect of boronization was lacking, stable discharges could only be produced at gas puff levels $\geq 3.8 \cdot 10^{22} \text{ atoms/s}$ and at a total heating power exceeding 6.8MW. Only within this reduced operational window could f_{ELM} be kept sufficiently high to allow an effective flushing of impurities necessary to avoid W accumulation. The two BL discharges (#28361 and #29958) in fig. 2 mainly differ in the number of discharges performed since the last boronization. Although the gas puff is twice as high in #29958 (21 days after boronization), f_{ELM} is just half of the value observed in #28361

(1 day after boronization). The gas puff rate of $3.8 \cdot 10^{22}$ atoms/s turned out to be the lower limit for the machine / wall condition of #29958, because it lead to ELMs ($f_{\text{ELM}} = 12\text{Hz}$) which are just frequent enough for an effective removal of impurities (in particular W) out of the pedestal. Thus, under such conditions only H-factors between 0.8 and 0.85 are possible. Attempts with a lower gas puff rate to improve the confinement produced even lower f_{ELM} and were terminated by W accumulation.

In ASDEX Upgrade, where nitrogen seeding is a common recipe for power load reduction, the first wall gets loaded with N. As a result, the intensity of a nitrogen N II emission line (399.5 nm) on an outboard limiter (4th box in fig. 2) - being a measure for the influx of an expected broad spectrum of medium-Z impurities from the wall - is a good indicator for the wall condition. Right after a boronization (#28361, in fig. 2), the N sticking on the wall is covered up and the level of this line is one order of magnitude smaller than in the case (#29958) where the effect of boronization is lacking. On AUG tungsten is mainly sputtered by medium-Z impurities from the main chamber wall [11]. Thus, the considerably different composition of the edge plasma with respect to low-Z impurities released by the first wall also has a significant impact on the tungsten concentration (c_{W} , see fig. 2) which is almost an order of magnitude larger in the case (#29958) where the effect of boronization is lacking. With the higher tungsten concentration also the core radiation level increases (see fig. 2) which leads to a decreasing ELM-frequency (f_{ELM}), because less power is crossing the separatrix. The ITER BL scenario on AUG is in particular sensitive to the quality of wall conditioning / closeness to boronization because the ELM-frequency already under good conditions is low and a further reduction by the described mechanism leads to insufficient impurity flushing of the pedestal by ELMs and finally to situation where central impurity accumulation cannot be avoided.

3. Possible optimization of the ‘operational point’

Since the operation at $q_{95} = 3$ and $\beta_{\text{N}} < 2$ turned out to be difficult in particular with respect to stationarity and the ELM behaviour, H-modes at the same toroidal field, but at lower I_{p} (higher q_{95}) were explored which still fulfil the requirement of $Q=10$. Keeping the fusion power $P_{\text{fus}} \sim (\beta_{\text{N}} / q_{95})^2$ and the fusion gain factor $G = Q / (Q+5) = 10.8 H_{98y2}^3 / (\beta_{\text{N}} \cdot q_{95}^2)$ [12] constant at the values of the ITER BL scenario, alternative values for H_{98y2} and β_{N} can be derived for a chosen q_{95} . Following this approach, target values for $\beta_{\text{N}} = 2.2$ and $H_{98y2} = 1.2$ are required for a chosen safety factor q_{95} of 3.6. As expected, lower values of I_{p} have to be

compensated by higher H-factors. At even higher q_{95} the requirements for H_{98y2} and for f_{GW} become unrealistically high, hence $q_{95}=3.6$ is selected. In order to avoid a hot divertor, a further assumption of keeping the same absolute edge density as for the current BL $q_{95}=3$ reference case, implies higher Greenwald fractions f_{GW} for the new alternative scenarios (at higher q_{95}). On AUG we have therefore explored the operational behaviour of plasmas at 2.0T / 1.0MA with a safety factor $q_{95} = 3.6$ in the ITER BL shape with target values of $\beta_N = 2.2$, $H_{98y2} = 1.2$ and $0.8 \leq f_{GW} \leq 0.95$. For ITER this would mean operation at 5.3T / 12.5MA instead of 5.3T / 15MA. This new alternative scenario and its comparison with the reference case, will give better insight into whether working at lower I_p is actually an advantage or leads to other operational problems due to the increased requirements for normalized confinement H_{98y2} and density f_{GW} .

4. Behaviour of the $q_{95}=3.6$ 'alternative ITER BL' discharges

In the following (see fig. 3) we compare an 'alternative' ITER BL discharge at 1.0 MA with a safety factor $q_{95} = 3.6$ to an ITER BL $q_{95}=3$ discharge at 1.2 MA. Both discharges are at the same toroidal field $B_t = 2T$. The applied heating power (NBI + ICRH) is kept the same, and the plasma shape is very similar. The NBI power at 3.6 MW (by reducing the beam voltage of one NBI box to 60 kV) has been chosen to achieve a normalized pressure β_N close to the target value of 1.8 for the $q_{95}=3$ case (#31146). With this reduced heating power (normally at full NBI beam voltage the NBI power for ITER BL demonstration plasmas at AUG is 5 MW leading to $\beta_N > 1.8$) impurity accumulation could only be avoided by using a high D_2 gas puff rate of $3.1 \cdot 10^{22} \text{ s}^{-1}$ although the discharge was performed shortly after a boronization. This gas puff level turned out to be sufficient to counteract the anticipated smaller ELM frequency caused by the reduction of the NBI heating power and has to be considered to be at the lower end to achieve stationary conditions.

For a comparison discharge at the lower $I_p = 1MA$ / higher $q_{95} = 3.6$ (#31148) the only parameter to choose was the gas puff rate. It turned out that at $q_{95} = 3.6$ this parameter ($1.5 \cdot 10^{22} \text{ s}^{-1}$) could be considerably smaller than in the $q_{95}=3$ case without losing stationarity of the plasma. Although plasma currents are different, the stored energy W_{MHD} in both discharges is the same (see fig. 3, upper, right box). The confinement factor H_{98y2} is 0.91 (at $\beta_N=1.87$) for $q_{95}=3$ and 1.05 (at $\beta_N=2.15$) for $q_{95}=3.6$. This increase in H-factor of 15% is promising, but the absolute value of 1.05 is below the target of 1.2. The absorbed heating power P_{net} is 30 - 40% above the H-mode power threshold (derived from scaling law, [13]).

The normalized pressure β_N is higher by 20% in the $q_{95}=3.6$ case. It was not possible to keep the plasma density fixed, but the Greenwald fractions f_{GW} of both discharges are almost identical and above the ITER target of 0.85 once the full shaping is reached after 3.2s. In the $q_{95}=3.6$ discharge (#31148) between 4.8s and 6s a magnetic perturbation (MP) $n=2$ field was switched on (indicated in both upper boxes of fig. 3) in order to test its influence on ELMs. Unfortunately the application of MP lead only to a degradation of both energy and particle confinement, but had no effect on ELMs.

In fig. 4 radial profiles of electron density and electron pressure averaged from 3.5s to 4.5s are shown for both discharges of fig. 3 (same colour code applies). Density profiles are almost flat. Central n_e values scale with the plasma current leading to identical f_{GW} . Electron temperatures are higher at the lower current leading to higher central electron pressure.

Scaling the plasma current down has provided a promising scenario at increased $q_{95}\sim 3.6$. Optimisation criteria are increasing central density by a further 15% and increasing H_{98y2} from 1.05 to 1.2. The main tools AUG has available to achieve this is an optimisation of particle fuelling by gas puff and pellets and the introduction of nitrogen for confinement improvement.

5. ELM mitigation attempts including Nitrogen seeding

In fig. 5 the normalized ELM energy loss ($\Delta W_{ELM} / W_{ped}$) is plotted versus the pedestal plasma collisionality. ELM energy loss values for both BL scenarios at $q_{95}=3$ and $q_{95}=3.6$ are compared with those of a multi-machine database compiled by Loarte [9] and exceed the general trend considerably. The observed large ELMs are intolerable and their mitigation / suppression is mandatory in view of ITER.

Therefore, three methods [7] for ELM mitigation were first tried in the $q_{95}=3$ ITER BL scenario: (i) ELM pace making with pellets ($v_p = 560$ m/s) of different mass ($m_p = 1.5 - 2.4 \cdot 10^{20}$ D atoms) and frequency (20-70 Hz) injected from the HFS, (ii) application of MP coils and (iii) nitrogen seeding.

In the all-W AUG pellet injection for pace making ceased to be a reliable ELM trigger [14] in purely D_2 fuelled plasmas. Therefore in such plasmas f_{ELM} never reached the pellet repetition frequency. However, recently it was found that the presence of N can recover the pellet ELM trigger potential [14]. In a N-seeded $q_{95}=3$ discharge - although at low δ and with more P_{NBI} (7.5MW) than typical for an ITER BL ($P_{NBI} \leq 5$ MW) plasma - pellets launched at rates ramped from 20 up to 47 Hz triggered ELMs reliably. A first attempt to apply such improved

triggering of ELMs by combining N seeding with pellet pacing at 70 Hz (#31151, $t > 4.0$ s) to the $q_{95}=3$ ITER BL scenario was conducted. In a phase 300ms before the first pellet was launched, N was introduced which reduced f_{ELM} from 17 to 10 Hz. In the 'pellet + N'-phase the D_2 puff rate was reduced by a factor of two to keep the total fuelling by D_2 puff and pellets similar to the previous phase with D_2 puffing only. In this 'pellet + N' phase some pellets triggered ELMs, others still failed to do so, leading transiently to a f_{ELM} of 50Hz. Surprisingly, this boost of f_{ELM} did not prevent impurity accumulation and density peaking. It seems that the optimal combination of puff rates for D_2 , N and the pellet parameters (mass, repetition rate) has not been found yet.

AUG's ELM suppression scenario with magnetic perturbation (MP) fields, which works above a certain density or collisionality threshold [15], should in principle be compatible with the ITER BL scenario. The application of MP coils in the ITER BL scenario slightly influenced both density and stored energy, but did not mitigate or even suppress ELMs. Although the required edge density for ELM suppression - found in another discharge with the same plasma shape (#29842), but at much higher $q_{95}=5.5$ - was reached, no mitigation of ELMs was observed. The reason for this might be the lower collisionality due to the lower q_{95} in the ITER BL case.

Seeding of N normally increases f_{ELM} and reduces the ELM size in AUG plasmas whereas in the few $q_{95}=3$ ITER BL attempts with N seeding f_{ELM} was in fact reduced. These discharges showed a slightly improved confinement, but were even more prone to W accumulation than purely D-puffed ones. So far, none of these three methods have led to a breakthrough in the $q_{95}=3$ ITER BL scenario.

These three methods for ELM mitigation were also applied to the $q_{95}=3.6$ scenario with similar results. In addition, phases with type-II ELMs were discovered in this scenario. In fig. 6 time traces of two $q_{95}=3.6$ discharges are compared which mainly differ by the z-position of the plasma or by the closeness to a double-null configuration which is measured by the d_{RXP} parameter. The latter is the separation between the two flux surfaces which define the two X-points at the outer midplane. By reducing this parameter in the phase of full shaping from 1.5 to 1 cm (see fig. 6) after $t=3$ s, type-I ELMs immediately disappear and a magnetic broad band signature appears typical for a type-II ELM scenario. Edge profiles do not significantly change, neither does energy and particle confinement. All empirical findings of these type-II ELMs are similar to previous type-II ELM studies at higher q_{95} [16] and to AUG results with a carbon wall [17].

Another step in d_{RXP} by 5mm after $t=4s$ reduces the energy confinement by 15%. A nitrogen puff in the final phase of the discharge ($5.6 < t < 6.2$) recovers energy confinement to an H-factor above 1. On AUG this well-known beneficial effect of nitrogen puffing on confinement at higher q_{95} and higher β_N [18] is here for the first time also clearly demonstrated for a $q_{95}=3.6$ plasma with ITER-like shape, but has to be considered in this case as a non-stationary effect, since both tungsten concentration and radiation are strongly increasing shortly after the introduction of nitrogen. However, until now only rather moderate D_2 and N gas puff levels were tried. The applied D_2 and N levels might not lead to sufficient edge cooling, but might just increase W-sputtering. Therefore, the successful examples [8, 18] of other discharges at higher q_{95} and higher β_N having higher levels of D_2 and N puffs will be tried during the next campaign in this $q_{95}=3.6$ scenario as well. In addition it will be tried to increase P_{ICRH} to counteract central impurity accumulation.

At first glance type-II ELMs seem to be a breakthrough for the development of a $Q=10$ scenario with small ELMs. Unfortunately, type-II ELM scenarios in present day machines are known to exist only at high collisionality and might be therefore in view of ITER of less interest. However at present knowledge it is not clear whether the collisionality at the pedestal or close to the separatrix is the decisive parameter for the stability of type-II ELMs. In the latter case the prospect to establish a type-II ELM scenario in ITER becomes more realistic, since the collisionality close to the separatrix in ITER does not significantly differ from the one in present day tokamaks like AUG.

6. Helium Operation

In order to simulate the ITER operation in the non-nuclear phase, helium discharges have been performed at AUG. For these experiments the operation at $B_T = 2.0T$ typical for D_2 ITER BL plasmas was given up, because ICRH is anyway not available at AUG for heating of He discharges. Lower values for current and field ($B_T = 1.4 / 1.8T$) were chosen in order to make the operation easier and to allow at the higher field the application of the ECRH X3 heating scheme. In addition, the operation at $0.8MA / 1.4T$ was also proposed with the idea to simulate at AUG the future half field operation in the ITER device. Since operation of the AUG NBI system with He was not possible at the time of the experiments, such He plasmas were heated with deuterium NBI and ECRH (1.1MA) or in the low I_p case (0.8MA) just with deuterium NBI. Thus, no 'pure' He operation on AUG was possible, but He concentrations of more than 70% were certainly reached. Although pumping of He in AUG is rather ineffective,

the operation of such He plasmas turned out to be unproblematic, once the appropriate (low) He puff level was found. Although the discharges were conducted more than 20 days after a boronization – a phase which was very challenging for operation of D₂ ITER BL plasmas – no major operational difficulties were observed.

This is demonstrated in particular in fig. 7 where two discharges at 0.8MA / 1.4T are compared, one is D₂ (red, #29977) fuelled the other one He fuelled (blue, 30011). At $B_t=1.4T$ no central wave heating is available. While D₂ discharges typically start to accumulate impurities (see tungsten concentration, c_w , upper, left box in fig. 7) under such wall conditions already at a time where the triangularity is still low, He discharges show a stationary behaviour with very low tungsten concentration c_w throughout the discharge. Around $t=2s$ both discharges have similar electron densities and temperatures. This is consistent with global stored energy W_{MHD} in D₂ $\sim 1.5 W_{MHD}$ in He (see fig. 7).

In fig. 8 time traces for a He discharge at 1.1MA / 1.8T are shown. In particular f_{ELM} was between 200 and 300 Hz and the dependency with δ is less pronounced compared to deuterium plasmas (e.g. fig1). High densities close to $f_{GW}=1$ were reached. Even the switch-off of central ECRH did not lead to W-accumulation.

The rising P_{rad} in fig. 8 is due to ECRF stray radiation (cut-off) disturbing the bolometer diagnostic rather than a sign of increasing core radiation. This interpretation is supported by the immediate reduction of P_{rad} once P_{ECRH} is zero and by the very low W concentration c_w , in particular in the phase with highest δ .

Typically in such He discharges, electron densities are close to the Greenwald limit, energy confinement is low ($H_{98y2} < 0.75$), f_{ELM} is high and triangularity does not have a significant impact on these parameters in contrast to the experience with deuterium plasmas. They even show stationary behaviour with unboronized walls and without centrally deposited wave heating which in the case of deuterium discharges is mandatory.

In order to demonstrate that lessons learned in non-activating He operation can be transferred to later D or even D-T operation in ITER, AUG will put more effort into the development of target plasmas with lower He fuelling and hence obtain lower ELM frequency such that ELM mitigation with MP and pellet pacing can also be demonstrated in such He plasmas.

7. Summary and Conclusions

At AUG-W several $q_{95}=3$ ITER BL demonstration discharges at $I_p=1.1$ and 1.2MA were performed with ECRH and ICRH and showed stationary behaviour for many confinement

times. Gas puffing rate and heating power are the parameters which have been varied in these discharges. The resulting values for H-factor, f_{GW} and β_N are shown in fig. 9. Values for normalized density f_{GW} and energy confinement H_{98y2} simultaneously came close to the requirements of the ITER BL scenario (see fig. 9) as long as β_N stayed above 2 (typically $2.0 < \beta_N < 2.2$). At a lower heating power and thus at $\beta_N = 1.8$ only H-factors around 0.85 have so far been achieved. Such low heated discharges were only stationary at D_2 puffing rates around $3 \cdot 10^{22}$ atoms/s and with a freshly boronized wall. The latter constraint is not a major problem for the extrapolation to ITER because boron-coated main chamber walls in AUG-W together with the tungsten divertor (typically not affected during a boronization process [10, 19]) simulate most closely the ITER situation of a Be main-chamber-wall and a tungsten divertor. The fact that in AUG-W no sufficient normalized confinement ($H_{98y2} \sim 1$) has been found at low heating power ($\beta_N = 1.8$) might be critical for ITER, since it suggests that significantly more additional heating would be required on this future device to achieve its goals. Previous results in AUG-C (see fig. 9) did not show this lack of confinement at low β_N . In AUG-C H-factors show only a much smaller decrease when heating power is reduced compared to the situation with metal walls in AUG-W. This different behaviour between AUG-C and AUG-W is certainly also due to the operational necessity (for stationary conditions) in AUG-W to choose the gas puff rate sufficiently high in order to flatten steep tungsten density gradients in the H-mode edge transport barrier by frequent ELMs. However, in ITER the neoclassical tungsten transport might even be outward drift dominated [20]. Therefore, the need to push ELM frequencies by high gas puff rates to tame the tungsten transport (as typical for AUG) might be no constraint for ITER operation, which will without doubt also have a beneficial effect on energy confinement.

As a possible alternative, the $q_{95}=3.6$ scenario has been investigated. The operational window allowing stationary behaviour at the higher safety factor is definitely larger compared to the $q_{95}=3$ scenario. Lower D_2 puff rates are possible even under conditions of a diminishing boronization. Discharges with high normalized densities f_{GW} and at the target β_N value of 2.2 have been established (see fig. 10). Normalized confinement in such discharges is above 1 but 12% below the target of $H_{98y2} = 1.2$. Thus also confinement has to be improved similar to the situation at $q_{95}=3.0$. This improvement might be achieved by N-seeding [18], which is a continuing topic of research. Also at JET with its ITER-like wall seeding of nitrogen in high- δ plasmas showed a beneficial effect on confinement [6, 21].

Very large ELMs, well above the established collisionality scaling [9], occurred in both scenarios, which appear difficult to mitigate. Three mitigation techniques (pellets, MP and N-seeding) have been tried, but did not show the desired effect. The solution for this problem remains the biggest challenge for optimizing such plasmas towards divertor heat load mitigation under steady-state conditions. As a side-result type-II ELM phases could be triggered by shifting the plasma closer to a double-null configuration. Seeding of nitrogen shows the first promising results in terms of improved confinement and reduced divertor temperature, but in both scenarios long-lasting stationary behaviour could not be reached until now.

The beneficial effect of higher triangularity to achieve simultaneously good confinement at high densities is similar in AUG-C and AUG-W (see left part of fig. 9) and thus confirms in this respect the choice for the ITER shape. A more detailed variation of the triangularity in other AUG plasmas reveals, that the density of the breakdown of the H-mode is not depending on the triangularity. However, the onset of the degrading H-mode phase is at a higher density for the higher triangularity, i.e. the H-mode phase with good confinement extends to higher densities [22].

However, higher triangularity is clearly also responsible for the occurrence of large low-frequency ELMs in these scenarios (see fig. 11) which are difficult to get rid of. Whether in total the ITER shape is a reasonable choice for an optimized ITER scenario cannot be answered at this stage. At least alternatives should be considered in case the large ELMs occurring in high triangularity ITER demonstration plasmas cannot be suppressed or mitigated in present-day machines.

Finally for the operation in helium no major difficulties were observed. During a recent AUG campaign the operation of ITER BL scenario in He was successfully extended towards lower densities and higher ELM frequencies. Results on these experiments will be published elsewhere [23] in the near future and will help to answer the important question for ITER whether ELM control with MPs developed in D_2 plasmas can be transferred to He plasmas and vice versa.

8. Acknowledgements

This work has been carried out within the framework of the EUROfusion Consortium and has received funding from the Euratom research and training programme 2014-2018 under grant

agreement No 633053. The views and opinions expressed herein do not necessarily reflect those of the European Commission.

9. References

- [1] SIPS, A.C.C., et al., 2012 Proc. 24th Int. Conf. on Fusion Energy (San Diego, 2012) <http://www-naweb.iaea.org/naweb/physics/FEC/FEC2012/index.htm>
- [2] SAIBENE, G. et al., Plasma Phys. Control. Fusion 44 (2002) 1769–1799
- [3] KESSEL, C.E. et al., Nucl. Fusion 53 (2013) 093021
[doi:10.1088/0029-5515/53/9/093021](https://doi.org/10.1088/0029-5515/53/9/093021)
- [4] JACKSON, G.L., et al., Nucl. Fusion 55 (2015) 023004
[doi:10.1088/0029-5515/55/2/023004](https://doi.org/10.1088/0029-5515/55/2/023004)
- [5] SIPS, A.C.C., et al., Nucl. Fusion 49 (2009) 085015
[doi:10.1088/0029-5515/49/8/085015](https://doi.org/10.1088/0029-5515/49/8/085015)
- [6] GIROUD, C. et al., Plasma Phys. Control. Fusion 57 (2015) 035004
[doi:10.1088/0741-3335/57/3/035004](https://doi.org/10.1088/0741-3335/57/3/035004)
- [7] SCHWEINZER, J., et al., Europhysics Conference Abstracts 37D (2013), P2.134
<http://eps2013.aalto.fi/?page=proceedings>
- [8] BEURSKENS, M., Plasma Physics and Controlled Fusion 55 (2013) 124043
[doi:10.1088/0741-3335/55/12/124043](https://doi.org/10.1088/0741-3335/55/12/124043)
- [9] LOARTE, A. et al 2003 Plasma Physics and Controlled Fusion 45 1549
- [10] ROHDE, V. et al., J. Nucl. Mat. 363-365 (2007) 1369-74
- [11] DUX, R., et al., J. Nucl. Mat 390-391 (2009) 858-863
- [12] PEETERS, A., et al., Nucl. Fusion 47 (2007) 1341–1345
- [13] RYTER, F., et al., Journal of Physics: Conference Series 123 (2008) 012035
[doi:10.1088/1742-6596/123/1/012035](https://doi.org/10.1088/1742-6596/123/1/012035)
- [14] LANG, P.T. et al., Nucl. Fusion 54 (2014), 083009
- [15] SUTTROP, W., et al., Phys. Rev. Lett. 106, 22 (2011), 225004
- [16] WOLFRUM, E. et al., Plasma Physics and Controlled Fusion 53, 8 (2011), 085026
- [17] STOBER, J. et al., Nucl. Fusion 41 (2001), 1123-1134
- [18] SCHWEINZER, J., et al., Nucl. Fusion 51 (2011) 113003
[doi:10.1088/0029-5515/51/11/113003](https://doi.org/10.1088/0029-5515/51/11/113003)
- [19] KALLENBACH, A. et al., J. Nucl. Mat. 363-365 (2007) 60-65
- [20] DUX, R., et al., *Europhysics Conference Abstracts (CD-ROM, Proc. of the 40th EPS Conference on Plasma Physics, Espoo, Finland, 2013)*, (Ed.) V. Naulin and C. Angioni and M. Borghesi and S. Ratynskaia and S. Poedts and T. Donné and T. Kurki-Suonio and S. Äkäslompolo and A. Hakola and M. Airila (European Physical Society, Geneva), Vol. 37D (2013), P4.143
- [21] GIROUD, C. et al., Nucl. Fusion 53 (2013) 113025
[doi:10.1088/0029-5515/53/11/113025](https://doi.org/10.1088/0029-5515/53/11/113025)
- [22] BERNERT, M. et al., Plasma Phys. Control. Fusion 57 (2015) 014038
[doi: 10.1088/0741-3335/57/1/014038](https://doi.org/10.1088/0741-3335/57/1/014038)
- [23] PÜTTERICH, T., private communication

Figures & Captions:

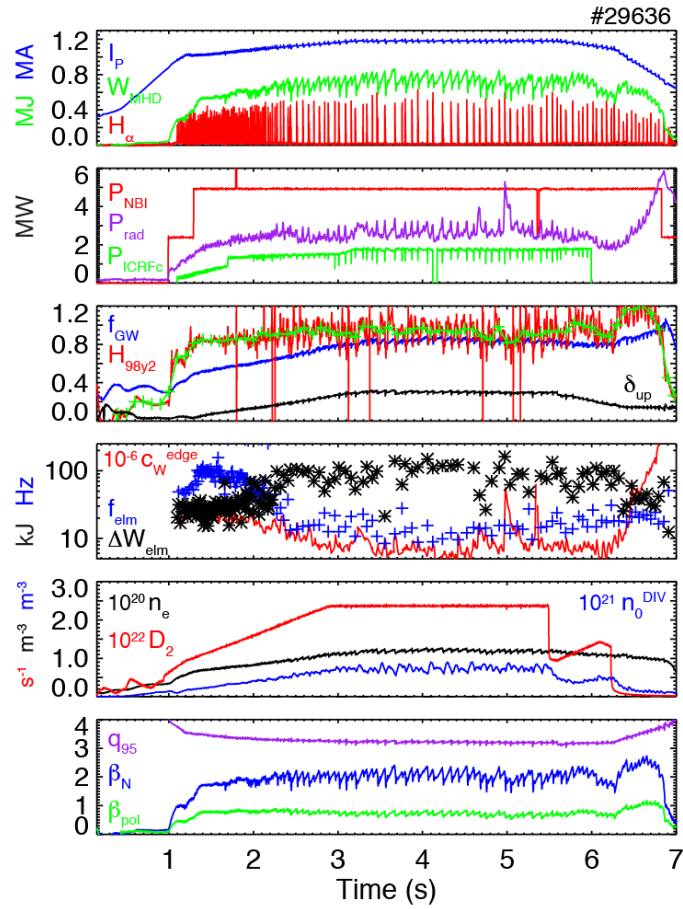


FIG. 1.: Time traces of 1.2MA / 2T ITER BL discharge (#29636) centrally heated by ICRH. Shown parameters: plasma current I_p , stored energy W_{MHD} , ELM signature H_α , neutral beam heating power P_{NBI} , ICRH power coupled to the plasma P_{ICRFc} , radiated power P_{rad} , Greenwald fraction f_{GW} , upper triangularity δ_{up} , H-mode factor H_{98y2} , tungsten concentration c_W^{edge} , ELM frequency f_{ELM} , energy loss per ELM ΔW_{elm} , line-averaged density n_e , deuterium puff rate D_2 , neutral gas density in the divertor n_0^{DIV} , safety factor q_{95} , normalized pressure β_N , beta poloidal β_{pol} .

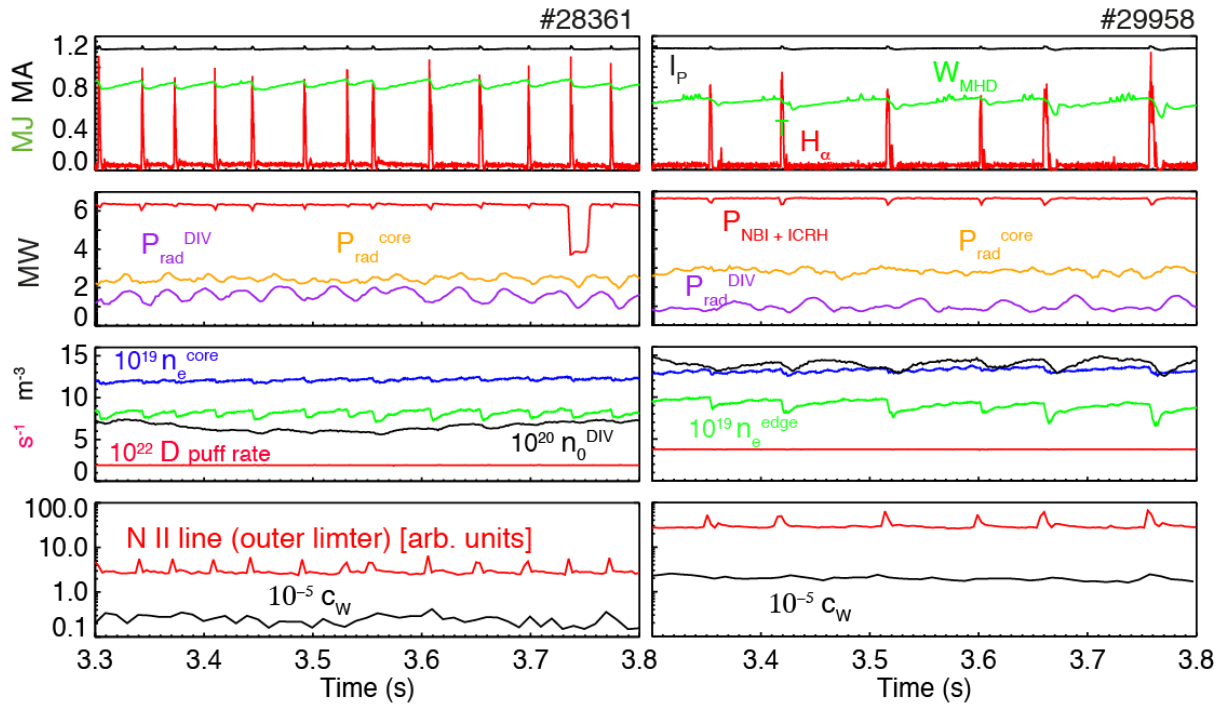


FIG. 2.: Comparison of ITER BL discharges during phases of 0.5s. Discharge parameters are identical except gas puff and ‘freshness’ of boronization. While the discharge on the left (#28361) was conducted 1 day after a boronization, the one on the right (#29958) was done 21 days after a boronization. Different gas puff levels $1.9 \cdot 10^{22}$ and $3.8 \cdot 10^{22}$ atoms/s were necessary to reach stationarity for discharges #28361 and #29958, respectively.

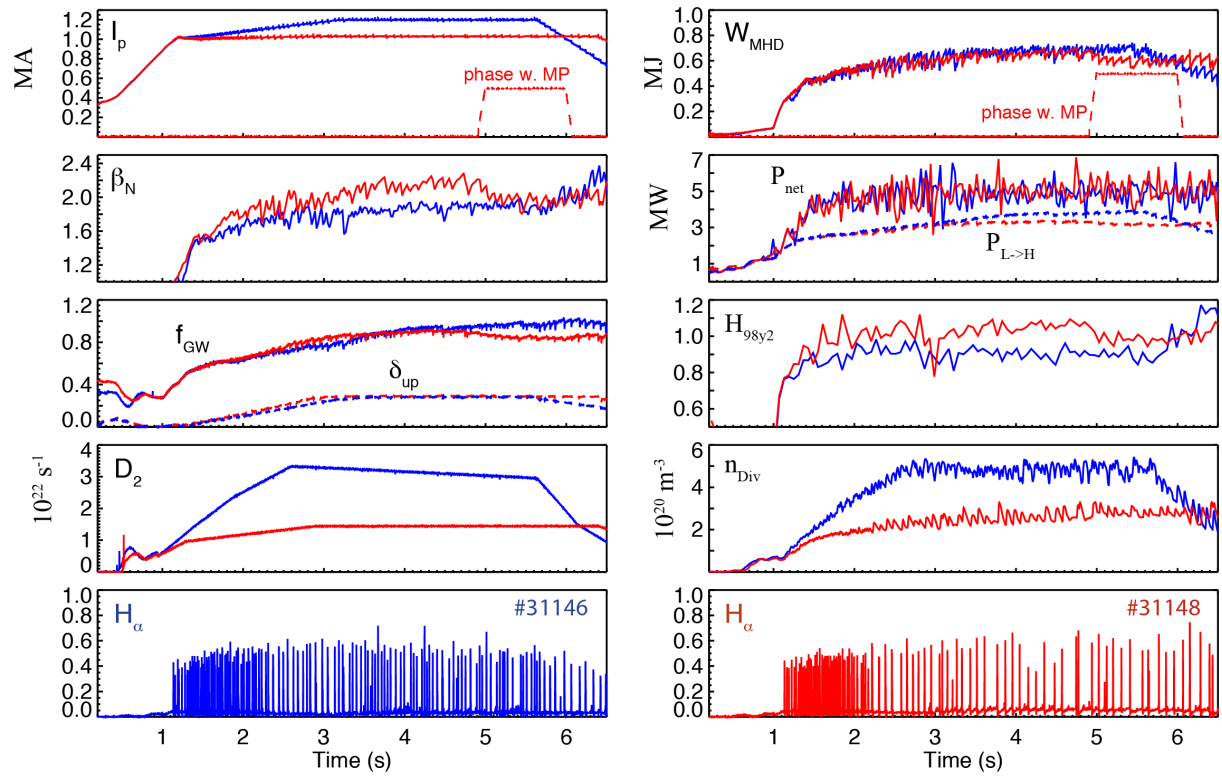


FIG. 3.: Time traces of various parameters (plasma current I_p , stored energy W_{MHD} , normalized pressure β_N , absorbed heating power P_{net} , H-mode power threshold $P_{L>H}$, Greenwald fraction f_{GW} , upper triangularity δ_{up} , H-mode factor H_{98y2} , D_2 puff rate, neutral gas density in the divertor n_{Div} , ELM signature H_α) for a comparison of a $q_{95}=3$ (#31146, blue) with a $q_{95}=3.6$ (#31148, red) discharge. For both discharges the toroidal field $B_t = 2\text{T}$, the applied heating power (NBI + ICRH) as well as the plasma shape are the same.

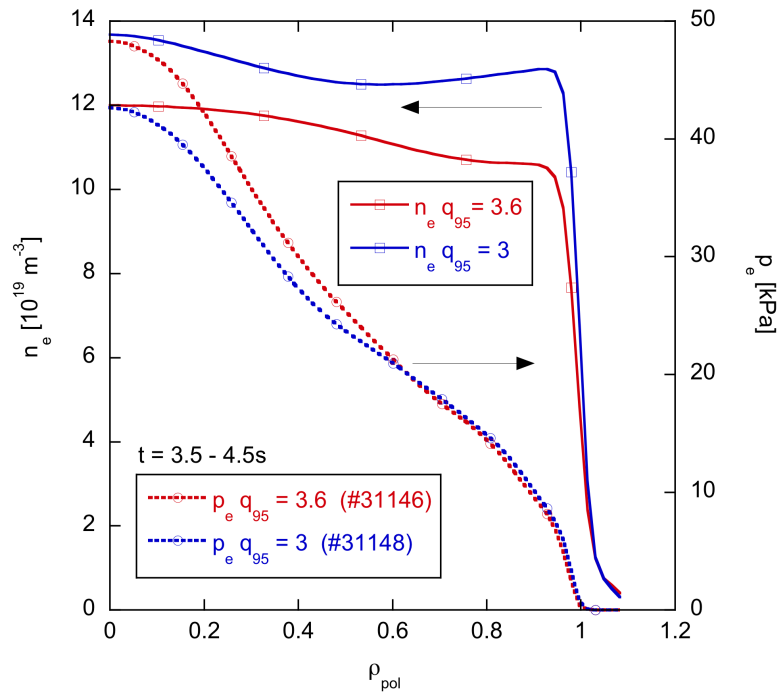


FIG. 4.: Radial profiles of electron density n_e and electron pressure p_e for the discharges of fig. 2 at $q_{95}=3$ (#31148, blue) and $q_{95}=3.6$ (#31146, red) averaged from 3.5s to 4.5s.

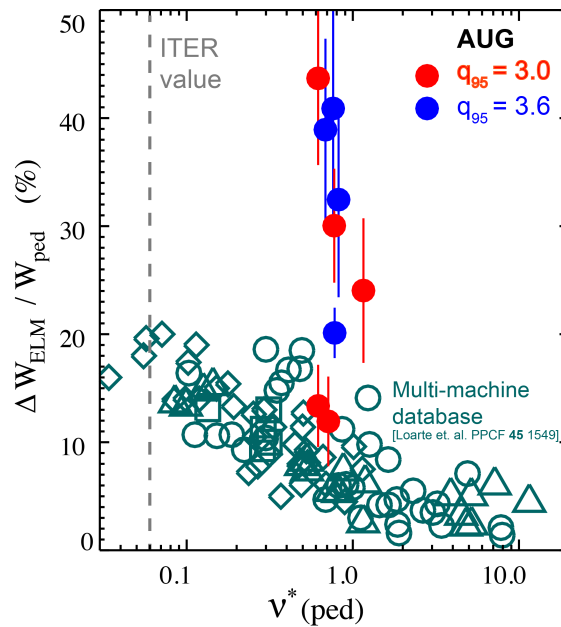


FIG. 5.: Energy loss of Type-I ELMs normalized to the pedestal stored energy vs. collisionality of the pedestal (value for ITER indicated by broken vertical line). Values for the two AUG scenarios at $q_{95}=3.0$ and $q_{95}=3.6$ are compared to a multi-machine scaling [9].

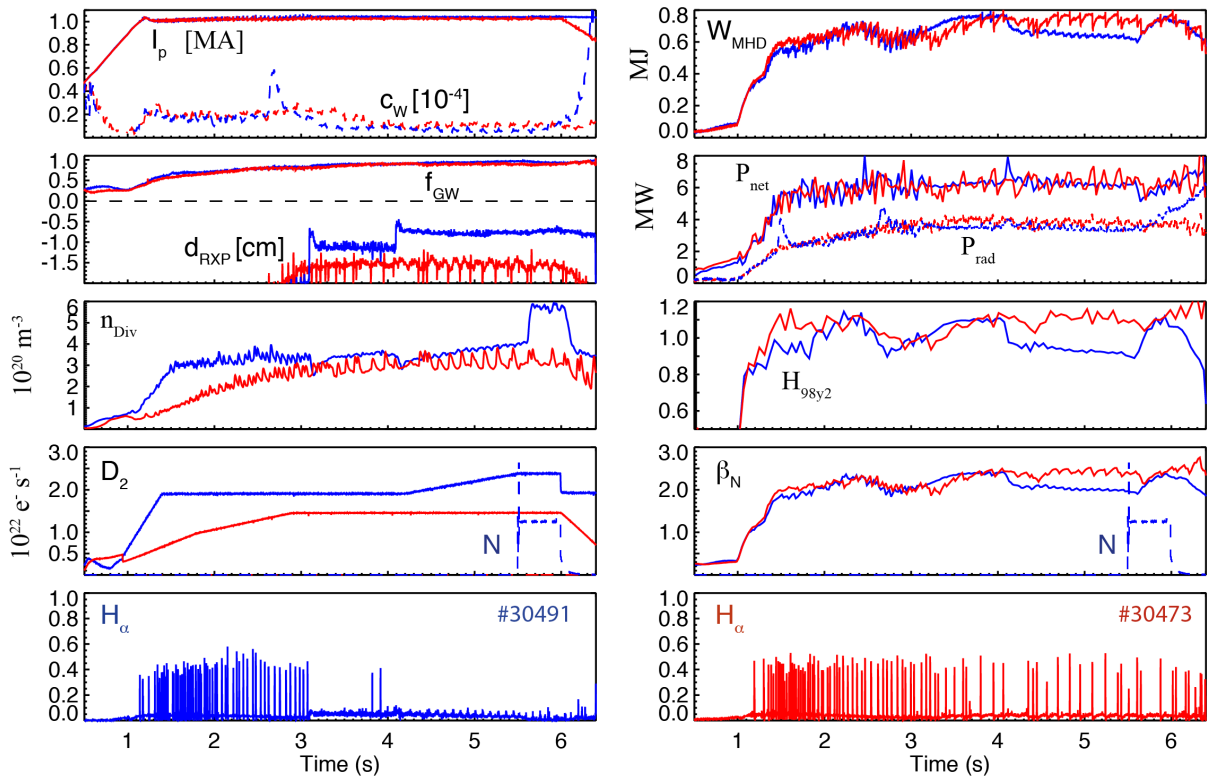


FIG. 6.: Time traces of various parameters (radiated power P_{rad} , separation of X-points d_{RXP} , nitrogen puff rate N) for two $q_{95}=3.6$ discharges (#30491 with a type-II ELM phase, blue;) with different closeness (d_{RXP}) to double-null configuration. For both discharges the toroidal field $B_t = 2\text{T}$, the applied heating power (NBI + ICRH) as well as the triangularity are the same.

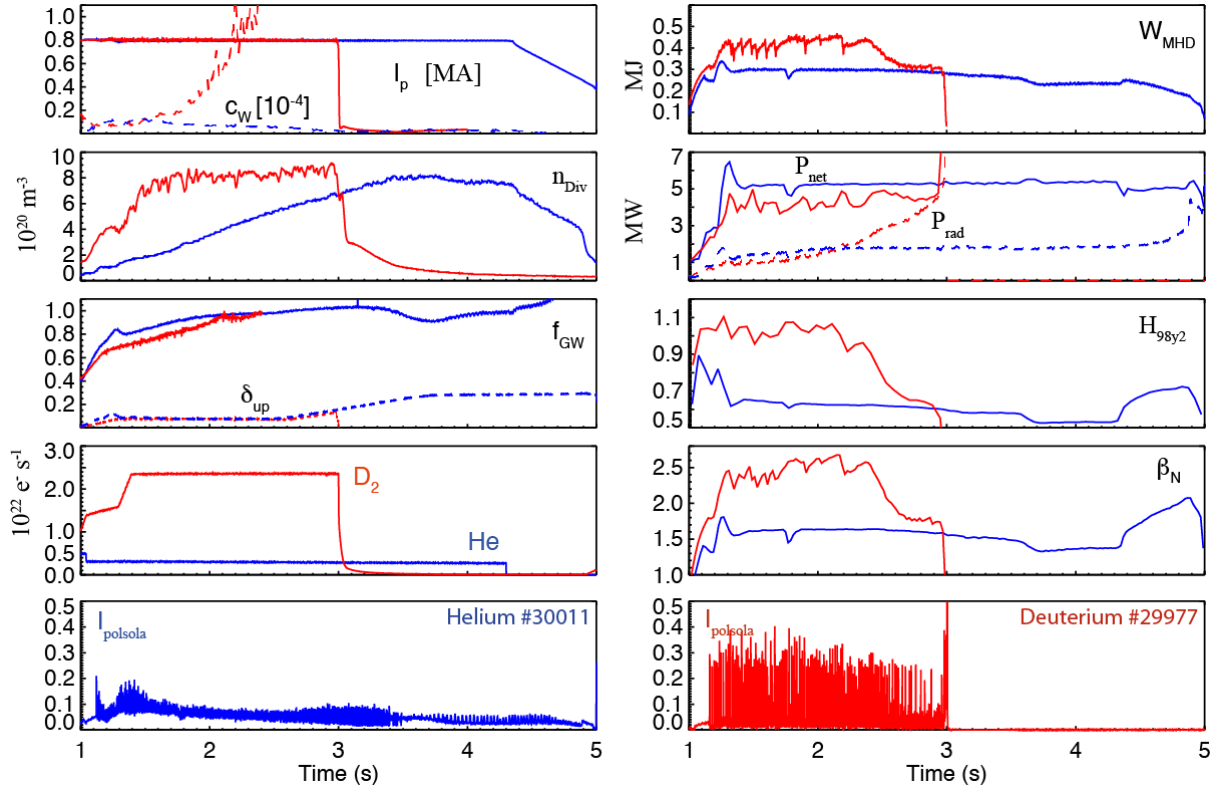


FIG. 7.: Time traces of various parameters (D_2 / He puff rate, $I_{polsola}$ poloidal currents from shunt measurements in the outer divertor target plates used as ELM signature) for a comparison of a $q_{95}=3$ He discharge (#30011, blue) with a $q_{95}=3$ D_2 (#29977, red) discharge. Other shown parameters: plasma current I_p , stored energy W_{MHD} , absorbed heating power P_{net} , radiated power P_{rad} , Greenwald fraction f_{GW} , upper triangularity δ_{up} , H-mode factor H_{98y2} , tungsten concentration c_w , neutral gas density in the divertor n_{Div} , normalized pressure β_N .

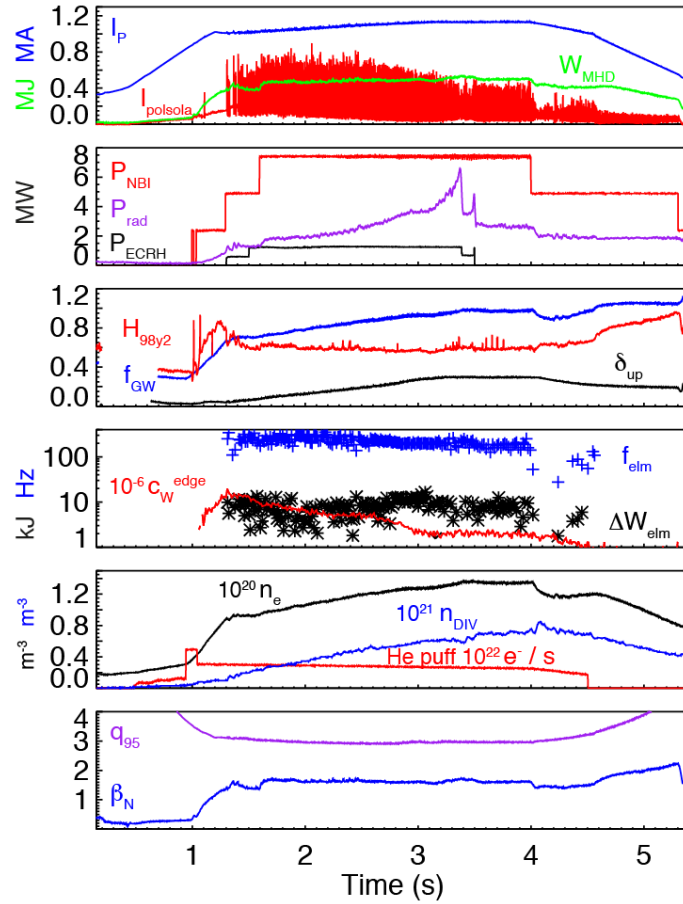


FIG. 8.: Time traces, of an ECRF-heated He discharge #30015 (1.1MA / 1.8T, further details, see text) Shown parameters: plasma current I_p , stored energy W_{MHD} , ELM signature $I_{polsola}$, neutral beam heating power P_{NBI} , ECRH power P_{ECRH} , radiated power P_{rad} , Greenwald fraction f_{GW} , upper triangularity δ_{up} , H-mode factor H_{98y2} , tungsten concentration c_W^{edge} , ELM frequency f_{ELM} , energy loss per ELM ΔW_{elm} , line-averaged density n_e , He puff rate, neutral gas density in the divertor n_{DIV} , safety factor q_{95} , normalized pressure β_N .

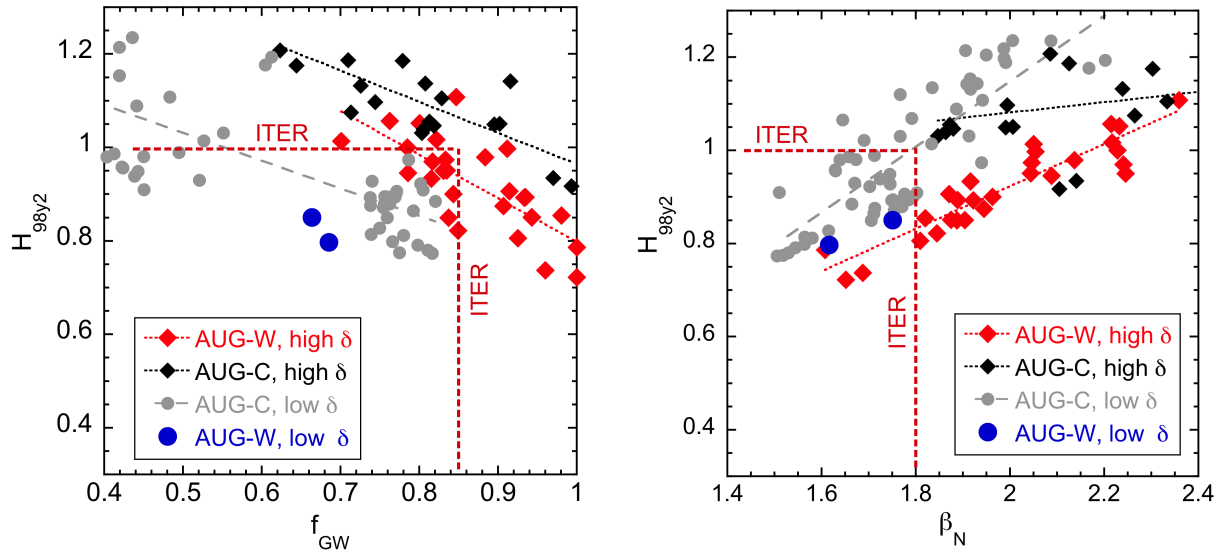


FIG. 9.: Normalized confinement H_{98y2} vs. density f_{GW} (left) and pressure β_N (right) for D_2 stationary operation at $q_{95} = 3$ in AUG-W and AUG-C at low and high triangularity. Parameters varied are gas puffing rate and heating power. Target values for the ITER BL scenario are indicated by red lines.

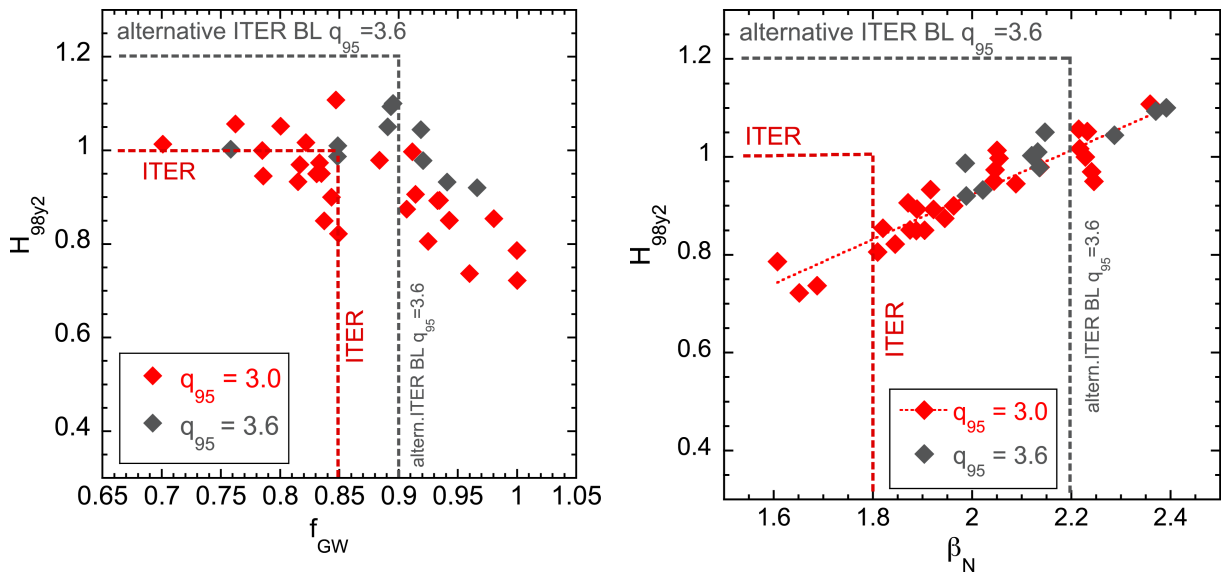


FIG. 10.: Normalized confinement H_{98y2} vs. density f_{GW} (left) and pressure β_N (right) for operation at $q_{95} = 3$ (red) and $q_{95} = 3.6$ (grey) in AUG-W (high δ). Target values for the ITER BL scenario and the alternative ITER BL scenario are indicated by red and grey broken lines, respectively.

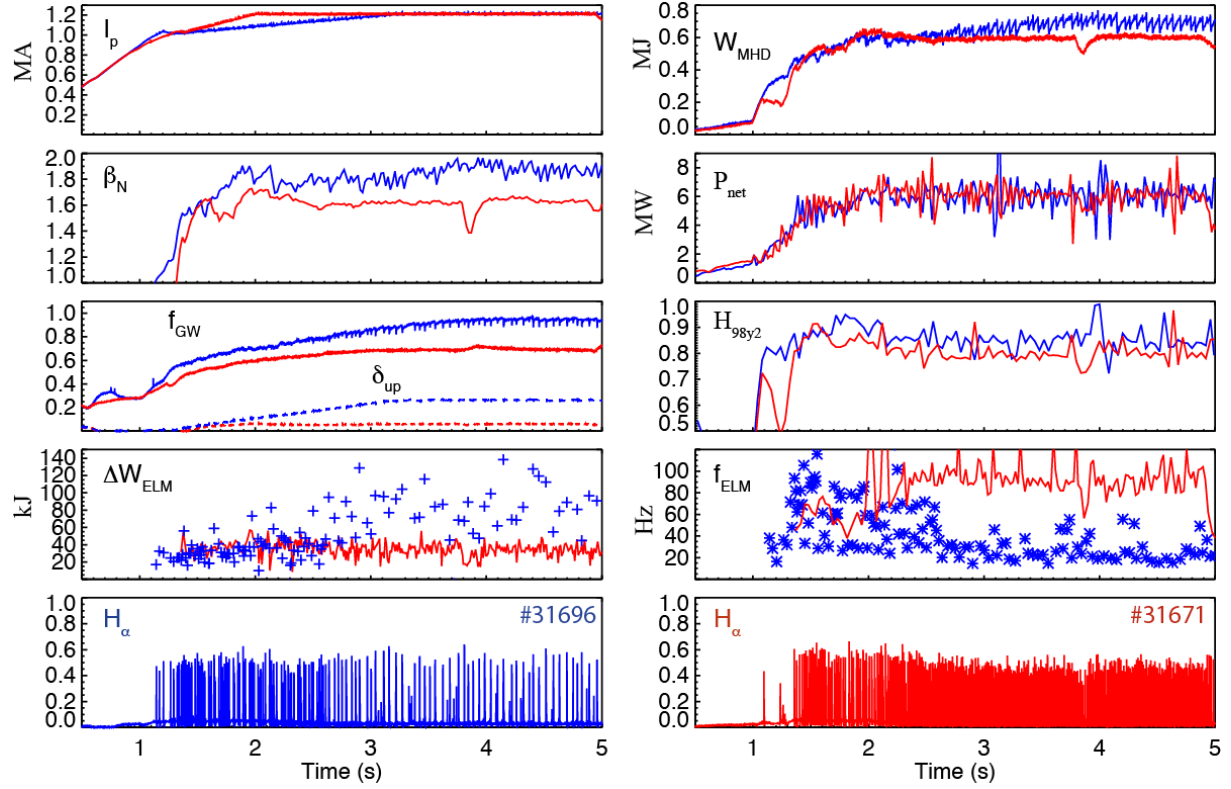


FIG. 11.: Time traces of various parameters (plasma current I_p , stored energy W_{MHD} , normalized pressure β_N , absorbed heating power P_{net} , Greenwald fraction f_{GW} , upper triangularity δ_{up} , H-mode factor H_{98y2} , energy loss per ELM ΔW_{ELM} , ELM frequency f_{ELM} , ELM signature H_α) for a comparison of a $q_{95} = 3.1$ (#31671, blue) discharge at high triangularity ($t > 3s$) with a $q_{95}=2.9$ (#31694, red) discharge at low triangularity. For both discharges the toroidal field $B_t = 2T$, the applied heating power (NBI + ICRH) as well as the high gas puff rate of $6 \cdot 10^{22} s^{-1}$ are the same.